



UNIVERSITY OF LEEDS

This is a repository copy of *Computational Efficient Personalised EMG-Driven Musculoskeletal Model of Wrist Joint*.

White Rose Research Online URL for this paper:

<https://eprints.whiterose.ac.uk/193399/>

Version: Accepted Version

---

**Article:**

Zhao, Y, Zhang, J, Li, Z [orcid.org/0000-0003-2583-5082](https://orcid.org/0000-0003-2583-5082) et al. (4 more authors) (2022) Computational Efficient Personalised EMG-Driven Musculoskeletal Model of Wrist Joint. IEEE Transactions on Instrumentation and Measurement, 72. 4001410. ISSN 0018-9456

<https://doi.org/10.1109/TIM.2022.3225023>

---

© 2022 IEEE. Protected by copyright. Personal use of this material is permitted. Permission from IEEE must be obtained for all other uses, in any current or future media, including reprinting/republishing this material for advertising or promotional purposes, creating new collective works, for resale or redistribution to servers or lists, or reuse of any copyrighted component of this work in other works.

**Reuse**

This article is distributed under the terms of the Creative Commons Attribution (CC BY) licence. This licence allows you to distribute, remix, tweak, and build upon the work, even commercially, as long as you credit the authors for the original work. More information and the full terms of the licence here:

<https://creativecommons.org/licenses/>

**Takedown**

If you consider content in White Rose Research Online to be in breach of UK law, please notify us by emailing [eprints@whiterose.ac.uk](mailto:eprints@whiterose.ac.uk) including the URL of the record and the reason for the withdrawal request.



[eprints@whiterose.ac.uk](mailto:eprints@whiterose.ac.uk)  
<https://eprints.whiterose.ac.uk/>

# Computational Efficient Personalised EMG-Driven Musculoskeletal Model of Wrist Joint

Yihui Zhao, Jie Zhang, *Member, IEEE*, Zhenhong Li, *Member, IEEE*, Kun Qian, Sheng Quan Xie, *Senior Member, IEEE*, Yu Lu, *Member, IEEE*, and Zhi-Qiang Zhang, *Member, IEEE*

**Abstract**—Myoelectric control has gained much attention which translates the human intentions into control commands for exoskeletons. The electromyogram (EMG)-driven musculoskeletal (MSK) model shows prominent performance given its ability to interpret the underlying neuromechanical processes among the musculoskeletal system. This model-based scheme contains inherent physiological parameters, e.g., isometric muscle force, tendon slack length, or optimal muscle fibre length, which need to be tailored for each individual via minimising the differences between the experimental measurement and model estimation. However, the creation of the personalised EMG-driven MSK model through the evolutionary algorithms is time-consuming, hurdling the use of the EMG-driven MSK model in practical scenarios. This paper proposes a computational efficient optimisation method to estimate the subject-specific physiological parameters for a wrist MSK model based on the direct collocation method. By constraining control variables to the experimentally measured EMG signals and introducing the physiological parameters into control variables, fast optimisation is achieved by identifying the discretised parameters at each grid simultaneously. Experimental evaluations on 12 healthy subjects are performed. Results demonstrate the proposed method outperforms the baseline optimisation algorithms used in the literature, including genetic algorithm, simulated annealing algorithm, and particle swarm optimisation algorithm. The proposed direct collocation method shows the possibility to alleviate the costly optimisation procedure and facilitate the use of the MSK model in practical applications.

**Index Terms**—EMG-driven musculoskeletal model, parameter optimisation, personalisation, direct collocation method, wrist joint.

## I. INTRODUCTION

MYOELECTRIC control has gained substantial attention in practical scenarios [1]–[4], such as increasing workers’ physical performance and preventing musculoskeletal disorders in industrial applications, or enhancing the patients’ recovery processes and restore the functional daily activities

This work was supported in part by U.K. EPSRC under Grant EP/S019219/1 and Grant EP/V057782/1, and in part by EU Marie Curie Individual Fellowship under grant 101023097. For the purpose of open access, the author(s) has applied a Creative Commons Attribution (CC BY) licence (where permitted by UKRI, ‘Open Government Licence’ or ‘Creative Commons Attribution No-derivatives (CC BY-ND) licence’ may be stated instead) to any Author Accepted Manuscript version arising.

Yihui Zhao, Jie Zhang, Zhenhong Li, Kun Qian, Sheng Quan Xie, and Zhiqiang Zhang are with the School of Electronic and Electrical Engineering, University of Leeds, Leeds, LS2 9JT, U.K. (e-mails: {eenyzhao, eenjz, z.h.li, fbskq, s.q.xie, z.zhang3}@leeds.ac.uk).

Sheng Quan Xie is also in collaboration with the Institute of Rehabilitation Engineering, Binzhou Medical University, Yantai, 264033, China.

Yu Lu is with the School of Educational Technology, Faculty of Education, Beijing Normal University, Beijing, China. (e-mail: luyu@bnu.edu.cn).

in rehabilitation applications. The myoelectric control decodes the human motion intention straightforwardly using the electromyogram (EMG) signal and encodes it into continuous control commands for controlling exoskeletons or prostheses [5]–[8].

To decode the human motion intention continuously, two main schemes are used, including the data-driven model [9], [10] and the musculoskeletal (MSK) model [11]. The data-driven model mostly employs regression algorithms, i.e., machine learning and deep learning algorithms, to establish the relationship between EMG signals and motion variables. However, the data-driven model is established based on numerical functions and abundant experimental data. It is essentially a “black-box” method where the underlying neuromechanical processes are omitted, limiting the use of the data-driven model in practical scenarios [12]. Alternatively, the MSK model explicitly interprets the non-linear transformation among the muscle activation, mechanical muscle forces, and motion variables. For instance, Jung *et al.* utilised the MSK model to estimate the ankle and knee joint torque during different walking conditions [13]. Bennett *et al.* also utilised the EMG-driven model to achieve accurate knee loading force prediction [14]. Nevertheless, the prediction performance of EMG-driven MSK models is substantially influenced by subject-specific parameters, i.e., maximum isometric force, optimal muscle fibre length, tendon slack length, and pennation angle, that define the force-generating capacity in the Hill’s muscle model. Since these parameters are difficult to estimate *in vivo* and they are closely related to gender, age, and activity levels, optimisation procedures are developed to establish the subject-specific EMG-driven MSK model [15].

The subject-specific MSK models are obtained through the objective functions that best match the experimental and estimated motion variables. Due to a large number of physiological parameters in the MSK model, the evolutionary algorithms are commonly employed such as the particle swarm optimisation (PSO) [16], [17], generic algorithm (GA) [18], [19], simulated annealing algorithm (SA) [20], and gravitational search algorithm (GSO) [21]. Nevertheless, it emerges that EMG-driven MSK models achieve the high estimation accuracy based on the expense of rapidity. Time-consuming optimisation procedures are reported to establish the personalised MSK model via evolutionary algorithms. For example, Silvestros *et al.* employed the genetic algorithm to obtain the optimal visco-elastic bushing parameters in a human cervical spine MSK model, which approximates a run time of 10 hours for each subject [18]. Sartori *et al.* also reported the

average optimisation time for the multiple degrees-of-freedom (DoFs) lower limb MSK model is around 20 hours [22]. Moreover, different calibration sets and multiple executions are also conducted to find the most optimal set of parameters. The time-consuming optimisation procedures, especially for the complex MSK model, impacts users' engagement and lead to barriers to the translation of the advanced MSK models into practical applications [23].

To address this issue, Buongiorno *et al.* proposed the linear optimisation approach that only optimises one parameter per muscle [24]. Although the linear approach is more computationally efficient, it fails to preserve the high estimation accuracy compared with the genetic algorithm. In addition, the personalised MSK model can be obtained through the direct collocation (DC) method. The DC method becomes a powerful approach paired with MSK models for predictive simulation [25], human movement analysing [26], and prosthesis control [27]. Falisse *et al.* employed the direct collocation method to estimate the subject-specific parameters for a lower limb MSK model which results in a short optimisation time and 30% improvement of the estimation performance, compared with the linear scaled method [28]. Nevertheless, there is no direct comparison with evolutionary algorithms that commonly used for the MSK models.

This paper builds on a previously published conference case study [29], in which the main goal was to present the preliminary validation of the DC method to estimate the subject-specific parameters on the limited subject samples using a limited set of performance criteria. This study develops the proposed DC method with enhanced accuracy and provides a rich comparison with the state-of-the-art evolutionary algorithms for the EMG-driven wrist MSK model. The contributions of this paper include: 1) The MSK model optimised by the proposed DC method achieves the same estimation performance as the MSK model obtained through evolutionary algorithms while the computation speed is significantly less than the evolutionary algorithms; 2) By taking account of the MSK dynamics and discretising the control and state variables, the wrist MSK model is transcribed into a large-scale non-linear programming (NLP) problem can be solved the NLP solver, IPOPT [30] effectively; 3) The physiological parameters are included as control variables, instead of as the static parameters, to improve the sparsity of the Jacobian matrix in the resultant NLP problem. A specific constraint is induced to maintain the parameters constant during the optimisation. Experimental evaluation is conducted on 12 healthy subjects. Three optimisation algorithms, including GA, SA, and PSO are selected as baseline methods to evaluate the proposed DC methods. Results indicate, under the same objective function and optimisation criteria, the proposed DC method outperforms the baseline methods in terms of the computational cost and estimation performance.

The remaining paper is organised as follows: Section II gives the methodology, including experiment protocols and the main framework of the proposed optimisation approach. Experimental results are presented in Section III. Finally, discussions are given in Section IV, followed by a conclusion in Section V.

## II. METHODS

### A. Experiment

Twelve subjects (eight males and four females, age  $28.9 \pm 2.8$  years) participant in the experiment with the given signed consent form. This experiment is approved by the MaPS and Engineering Joint Faculty Research Ethics Committee of the University of Leeds (MEEC 18-002). Each subject is informed to seat on an armchair and 16 reflective markers are placed on the right arm, corresponding to the VICON upper limb model. The markers' trajectories are recorded through the 8 VICON motion capture cameras (sampled at 250 Hz) and the motion data are low-pass filtered (Butterworth  $2^{nd}$ , 1 Hz). The wrist kinematics are then computed through the VICON nexus software.

EMG signals are recorded using the Delsys Trigno<sup>TM</sup> system (sampled at 2000 Hz). Five wireless electrodes are placed over two wrist flexors (*flexor carpi radialis* (FCR), *flexor carpi ulnaris* (FCU)), and three wrist extensors (*extensor carpi radialis longus* (ECRL), *extensor carpi radialis brevis* (ECRB), and *extensor carpi ulnaris* (ECU)). The electrodes' positions are determined by the palpation and evaluation of the signal quantify prior to the experiment. Raw EMG signals are band-pass filtered (Butterworth  $4^{th}$  order, 25 Hz - 450 Hz), fully rectified, and low-pass filtered (Butterworth  $4^{th}$  order, 4 Hz). The resultant signals are normalised with respect to maximum voluntary contraction (MVC) that are measured prior to the experiment. All data are synchronised and resampled at 1000 Hz.

During the experiment, subjects are informed to perform the continuous wrist flexion/extension motion. Five repetitive trials are obtained for each subject. A three-minute break is given between trials to prevent muscle fatigues.

### B. Wrist MSK Model

The wrist MSK model is utilised to compute the wrist flexion/extension motion through five muscle-tendon actuators ( $i = 1, 2, \dots, 5$ ) that correspond to wrist muscles selected in the study. The wrist MSK model includes activation dynamics and contraction dynamics. The activation dynamics contain a first-order differential equation to compute the neural activation  $a$  relating to the filtered signal  $e_i$ , which can be written as [31]:

$$\frac{da_i}{dt} = \left( \frac{e_i}{t_{act}} + \frac{1 - e_i}{t_{deact}} \right) (e_i - a_i) \quad (1)$$

where the  $t_{act}$  and  $t_{deact}$  denote the activation time and deactivation time, which are set to 15 ms and 50 ms respectively. Moreover, the activation dynamics are augmented by:

$$a_i^{non} = \frac{e^{Aa_i} - 1}{e^A - 1} \quad (2)$$

where  $a_i^{non}$  is the resultant muscle activation. The  $A$  denotes the coefficient to account for the non-linearity.

Contraction dynamics used in this study are described by the rigid musculotendon model [32], in which the pennated muscle element, comprising a contractile element in parallel with a passive elastic element, is connected to an inextensible

tendon element. Thus, the muscle-tendon force is calculated by [33]:

$$F_{mt,i} = F_{iso,i}(f_a(\hat{l}_m))f(\hat{v}_m)a_i^{non} + f_p(\hat{l}_m) \cos \phi_i \quad (3)$$

$$l_{mt,i} = l_{m,i} \cos \phi_i + l_{ts,i} \quad (4)$$

where  $F_{iso,i}$  denotes the maximum isometric force. The  $f_a(\hat{l}_m)$ ,  $f(\hat{v}_m)$ ,  $f_p(\hat{l}_m)$  interpret the force-length-velocity characteristics relating to the  $a_i^{non}(t)$ , normalised muscle length  $\hat{l}_m = l_{m,i}/l_{mo,i}$ , and  $f(\hat{v}_m)$ . In this study, we set  $f(\hat{v}_m) = 1$ , according to [34]. To update the muscle length (Eq. (4)), the muscle-tendon lengths  $l_{mt,i}$  are approximated by the second-order Fourier equation with respect to wrist joint angle  $\theta$ , which are exported from OpenSim [35].

To estimate the wrist joint motion, we model the hand as a rigid segment which is rotated around the wrist joint in the sagittal plane. The wrist joint angle is then computed by forward integration of the equation of motion:

$$M\ddot{\theta} + C\dot{\theta} + K\theta = \tau \quad (5)$$

where  $\theta$  denotes wrist joint angle.  $M$  denotes the mass term which is estimated based on the subject's body mass and height [36].  $C$  and  $K$  denote the damping and stiffness term respectively, according to [37].  $\tau$  is the joint torque estimated from the wrist MSK model:

$$\tau = \sum_{i=1}^5 \frac{\partial l_{mt,i}}{\partial \theta} F_{mt,i} \quad (6)$$

1) *Parameter Optimisation:* The wrist MSK model contains muscle-related physiological parameters that need to be tailored for each subject, including the isometric muscle force  $F_{iso,i}$ , optimal muscle length  $l_{mo,i}$ , and tendon slack length  $l_{ts,i}$ . To further account for the inter-subject variation, we induce the scale coefficient  $k_i$  for the muscle-tendon length. The EMG-to-activation coefficient  $A$  is a single parameter. We then use a vector  $\mathbf{p}$  to collect all parameters:

$$\mathbf{p} = [F_{iso,i}, l_{mo,i}, l_{ts,i}, k_i, A] \quad (7)$$

The estimation of  $\mathbf{p}$  can be written as:

$$\hat{\mathbf{p}} = \arg \min_{\mathbf{p}} \{J\} \quad (8)$$

where

$$J = \frac{1}{T} \sum_{t=1}^T (\theta_t - \hat{\theta}_t)^2 \quad (9)$$

where  $\theta$  and  $\hat{\theta}$  denote the ground truth and estimated value respectively.  $T$  denotes the total sample number.

The resultant parameter optimisation problem (Equation (8)) is solved by evolutionary algorithms such as GA, SA, and PSO. However, this commonly leads to a time-consuming optimisation procedure [24]. In the next section, we will present a computationally efficient manner to determine these parameters using the DC method.

### C. Direct Collocation Method

To optimise the physiological parameters through the DC method, we first convert the wrist MSK model into an optimal control problem that finds control variable  $\mathbf{u}$  and state variable  $\mathbf{x}$  to minimise the objective function. The DC method is then utilised to transcribe the optimal control problem into a finite-dimension NLP problem, which discretises the control and state variables and utilises the system dynamics as the constraints [38]. Thus, the optimisation problem can be formulated as:

$$\min_{\mathbf{u}, \mathbf{x}} J \quad (10)$$

subject to

$$\mathbf{f}(\mathbf{x}, \dot{\mathbf{x}}, \mathbf{u}) = 0 \quad (11)$$

$$\mathbf{U}_{lo} \leq \mathbf{x}, \mathbf{u} \leq \mathbf{U}_{up} \quad (12)$$

where  $\mathbf{x}$  and  $\mathbf{u}$  denote the state and control variables.  $\mathbf{f}(\mathbf{x}, \dot{\mathbf{x}}, \mathbf{u})$  denotes the system dynamics.  $\mathbf{U}_{lo}$  and  $\mathbf{U}_{up}$  are the boundary conditions, which are entailed in Table I.

The control variables contains the filtered EMG signal  $e_i$  and the physiological parameters:

$$\mathbf{u} = [e_i, \mathbf{p}]. \quad (13)$$

The physiological parameters are considered as control variables, instead of the static parameters, in order to enhance the sparse pattern of the Jacobian matrix, as depicted in Fig. 1. The state variables encompass the joint angle  $\theta$ , joint velocity  $v$  and muscle activation  $a_i(t)$ , which are represented by:

$$\mathbf{x} = [\theta, v, a_i]. \quad (14)$$

Equations (1), (3), (5), and (6) are utilised to impose the system dynamics  $\mathbf{f}(\mathbf{x}, \dot{\mathbf{x}}, \mathbf{u})$ . We use the implicit formulation in this study:

$$\mathbf{f}(\mathbf{x}, \dot{\mathbf{x}}, \mathbf{u}) = \begin{cases} \dot{\theta} - v \\ M\dot{v} + Cv + K\theta - \tau \\ \dot{a}_i - (e_i - a_i)\left(\frac{e_i}{t_{act}} + \frac{1-e_i}{t_{deact}}\right) \end{cases} \quad (15)$$

where  $\dot{\theta}$ ,  $\dot{v}$ , and  $\dot{a}_i$  denotes the derivatives of the state variables. The related optimal control problem is then transcribed into the finite-dimension NLP problem by discretising the state variables  $\mathbf{x}$  and control variables  $\mathbf{u}$  on  $Y$  equal-spaced grids. We use the same objective function  $J$  in the DC method. Moreover, the system dynamics are converted into the algebraic equality constraints using the finite differential approximation, where the mid-point rule is used:

$$\mathbf{f}\left(\frac{\mathbf{x}_{n+1} + \mathbf{x}_n}{2}, \frac{\mathbf{x}_{n+1} - \mathbf{x}_n}{t_{n+1} - t_n}, \frac{\mathbf{u}_{n+1} + \mathbf{u}_n}{2}\right) = 0, \quad (16)$$

$$n = 1, 2, 3 \dots Y - 1;$$

The initial conditions of control and state variables are consistent with the measured EMG signal and wrist joint motion, resulting in seven task constraints. Since the physiological parameters are added as control variables, we utilised specific equality constraints to restrict these parameters are invariant at each discretised grid:

$$\mathbf{p}_{n+1} - \mathbf{p}_n = 0 \quad (17)$$

The default value of the muscle-tendon parameters is taken from [39], as depicted in Table I. The pennation angle is excluded as it has the negligible effects on the prediction performance [40]. Moreover, to make  $e_i$  is consistent with the measured EMG signals, the upper and lower boundaries for  $e_i$  are equal to measured EMG signals. The resultant boundary conditions are also reformulated to have the same length as the discretised control and state variables.

TABLE I  
BOUNDARY CONDITIONS FOR CONTROL AND STATE VARIABLES

p	Muscle	Default	Boundary	p	Muscle	Default	Boundary
$F_{iso}$	FCR	407.9	$\pm 50\%$	$l_{mo}$	FCR	0.063	$\pm 15\%$
	FCU	479.8			FCU	0.051	
	ECRL	337.3			ECRL	0.081	
	ECRB	252.5			ECRB	0.059	
	ECU	192.9			ECU	0.062	
p	Muscle	Default	Boundary	p	Muscle	Default	Boundary
$l_{ts}$	FCR	0.244	$\pm 15\%$	k	FCR	1	$\pm 15\%$
	FCU	0.265			FCU	1	
	ECRL	0.244			ECRL	1	
	ECRB	0.222			ECRB	1	
	ECU	0.229			ECU	1	
A		-2	[-3,0.001]	a		0	[0,1]
$\theta$		0	[-70,70]	v		0	[-inf, inf]

1) *Implementation*: The MSK model-related optimal control problem for the DC method contains 7 states variable (2 joint kinematics and 5 muscle activations), and 26 control variables (5 filtered EMG signals and 21 muscle-tendon parameters), which leads to a total  $Y \times (7 + 26)$  unknown parameters. The total number of the equality constraints is  $(Y - 1) \times (7 + 21) + 7$ . We set  $Y = 200$  in this study.

The resultant NLP problem can be solved by a standard NLP solver, IPOPT, which is available in the MATLAB platform. We utilise the IPOPT solver with the Hessian matrix approximation. Moreover, the NLP solver requires the gradient of the objective function and the Jacobian of constraints. We manually generate the sparse patterns of the constraint Jacobian matrix with respect to the discretised vector using the MATLAB symbolic toolbox, as illustrated in Fig. 1. The proposed DC method is available online: [github.com/eenyzhao/DC-code](https://github.com/eenyzhao/DC-code).

#### D. Baseline methods

In this study, we compare the proposed DC method with three baseline methods that are used for the MSK optimisation, including GA, SA, and PSO. The evolutionary algorithms are performed using the MALTAB optimisation toolbox (*ga*, *simulannealbnd*, and *particleswarm*). In the optimisation criteria (*options*), the tolerance for all evolutionary algorithms is set to  $1 \times 10^{-2}$ . Moreover, the optimisation termination (*MaxStallIterations*) are set to 51, 20, 2000 for the GA, PSO, and SA. The *MaxIterations* are set to 1000, 1000, 10000 for GA, PSO, and SA. Other settings remain default. For the DC method, the *convergence tolerance* and *constraints tolerance* are set to  $1 \times 10^{-2}$  and  $1 \times 10^{-3}$  respectively. The most optimal solution for each approach is then selected.

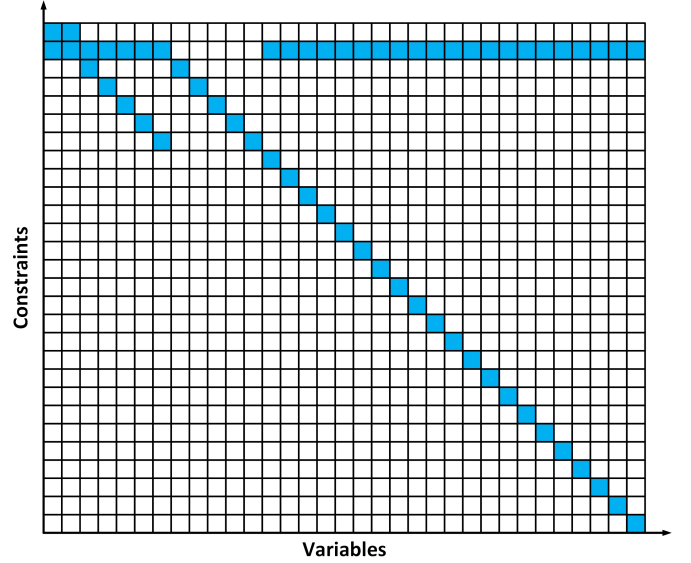


Fig. 1. The partial derivatives of constraints function with respect to state and control variables results in the sparse Jacobian matrix containing 61 non-zero elements at each grid. Columns correspond the state and control variables and rows correspond to the constraints functions.

#### E. Performance Criteria

To obtain the subject-specific muscle-tendon parameters, a cycle of wrist flexion/extension movement is extracted from the experimental trial for each subject. The remaining motion trials are used to validate the feasibility of the optimal solution. Two criteria are used to evaluate the estimation performance, root mean square error (RMSE) and coefficient of determination ( $R^2$ ):

$$\text{RMSE} = \sqrt{\frac{1}{T} \sum_{t=1}^T (\theta_t - \hat{\theta}_t)^2} \quad (18)$$

$$R^2 = 1 - \frac{\text{Var}(\theta - \hat{\theta})}{\text{Var}(\theta)} \quad (19)$$

In particular, RMSE and  $R^2$  reveal the difference in terms of amplitude and correlation between the estimation and the ground-truth, respectively. To evaluate the computational cost, the optimisation duration of each optimisation is measured.

Separate one-way analysis of variance (ANOVAs) are conducted. The performance criteria are used as the response variables. Moreover, a post-hoc analysis using Tukey's Honest Significant Difference test is applied. The significance level is set at  $p < 0.05$ .

### III. RESULTS

In this section, we verify the feasibility and effectiveness of the proposed DC method to estimate the subject-specific parameters for the wrist MSK model. In specific, the overall comparisons with baseline methods are carried out in terms of the computational cost and estimation accuracy. Subsequently, detailed evaluations are presented to demonstrate the robustness of the proposed method against the grid densities and different initial guesses. All optimisation algorithms are

performed on the same laptop computer with 2.6 GHz Intel i5-1145G7 CPU and 16 GB of RAM, running on MATLAB R2019a and IPOPT release 3.14.4.

### A. Overall Comparison

We first evaluate the computational cost of all optimisation algorithms. Fig. 2 elucidates the optimisation duration vs. iterations in four optimisation algorithms. It is found that GA (11.65) has the largest slope, followed by PSO (10.24). The SA (0.257) has the similar slope with the proposed DC (0.263). However, the SA requires larger number of iterations to find the optimised physiological parameters. Fig 3 illustrates the optimisation duration for each subject, which demonstrates the SA required longer time to find the optimal solution. It emerges that the proposed method can identify the optimised parameters in a computational-efficient manner.

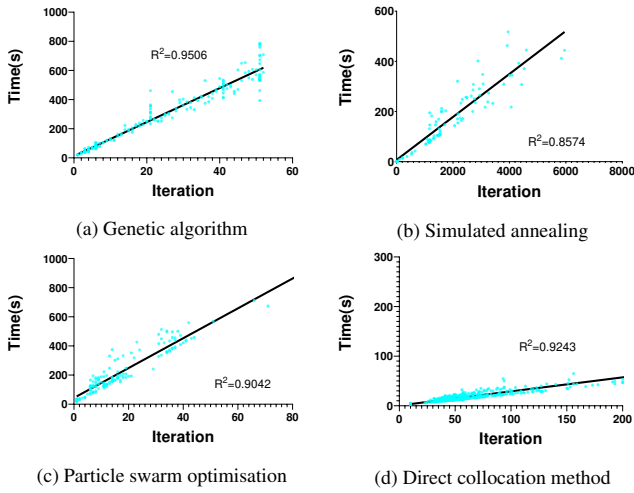


Fig. 2. The optimisation duration against the iterations for four optimisation algorithms. The slopes are 11.65, 0.2575, 10.24, and 0.2832 for GA, SA, PSO, and DC respectively.

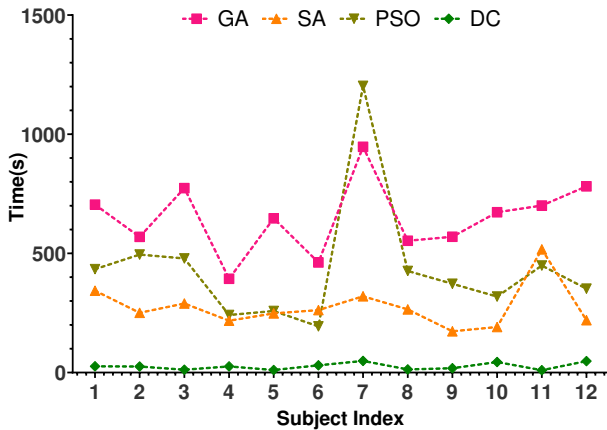


Fig. 3. Comparison of the optimisation time across subjects. The time cost of the DC method is the smallest among subjects.

We then evaluate the estimation performance for all optimisation algorithms. The mean  $R^2$  and RMSE of all optimisation algorithms are given in Table II and Fig. 4. There

TABLE II  
THE MEAN (STANDARD DEVIATION)  $R^2$  AND RMSES OF BASELINE APPROACHES AND THE PROPOSED DC METHOD.

	GA	SA	PSO	DC
$R^2$	0.852( $\pm 0.081$ )	0.837( $\pm 0.064$ )	0.868( $\pm 0.064$ )	0.880( $\pm 0.049$ )
RMSE (rad)	0.210( $\pm 0.082$ )	0.223( $\pm 0.084$ )	0.198( $\pm 0.077$ )	0.191( $\pm 0.072$ )
Duration (s)	648.07( $\pm 150.87$ )	274.912( $\pm 90.89$ )	435.24( $\pm 260.56$ )	26.06( $\pm 14.35$ )

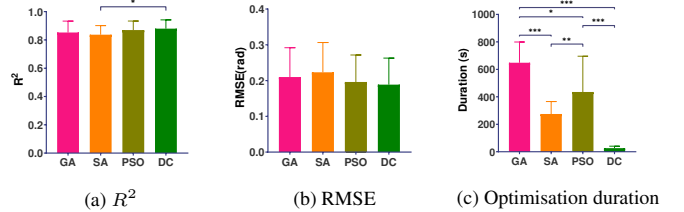


Fig. 4. The estimation accuracy and computational cost of the wrist MSK model via different optimisation algorithms. The proposed DC method achieves the same performance as the baseline methods while the optimisation cost is the smallest. The significance level is set as 0.05 (\*\* $p < 0.01$ , \*\*\* $p < 0.001$ , and \* $p < 0.05$ ).

is a significant difference between the DC method and SA regarding the  $R^2$  ( $p = 0.013$ ). Moreover, one representative result is given in Fig. 5, in which the subject-specific parameter estimated by the DC method results in a higher  $R^2$  and a smaller RMSE compared with baseline methods. It emerges that the DC method reaches the same precision compared with the GA, SA, and PSO. Therefore, to a large extent, it can find a better solution to the subject-specific parameters for the wrist MSK model under the same objective function and optimisation criteria.

We further measure the mean optimisation duration to estimate the subject-specific parameters under the same optimisation criteria, which is depicted in Table II and Fig. 4(c) respectively. The duration of the optimisation procedure of the DC method is 26.06 s ( $\pm 14.35$  s), which is significantly less than the baseline methods. Post-hoc analyses indicate the proposed approach is more statistically efficient than the baseline methods.

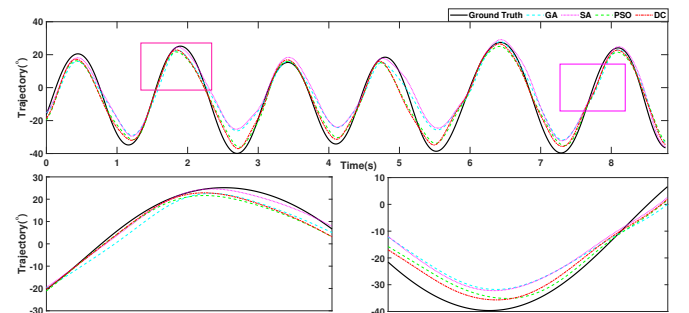


Fig. 5. Representative example indicates that the proposed approach achieves the same accuracy with the baseline optimisation approaches. In specific,  $R^2$  are 0.872, 0.864, 0.918, and 0.927 for GA, SA, PSO, and DC respectively. RMSEs are 0.132 rad, 0.137 rad, 0.106 rad, and 0.10 rad respectively.

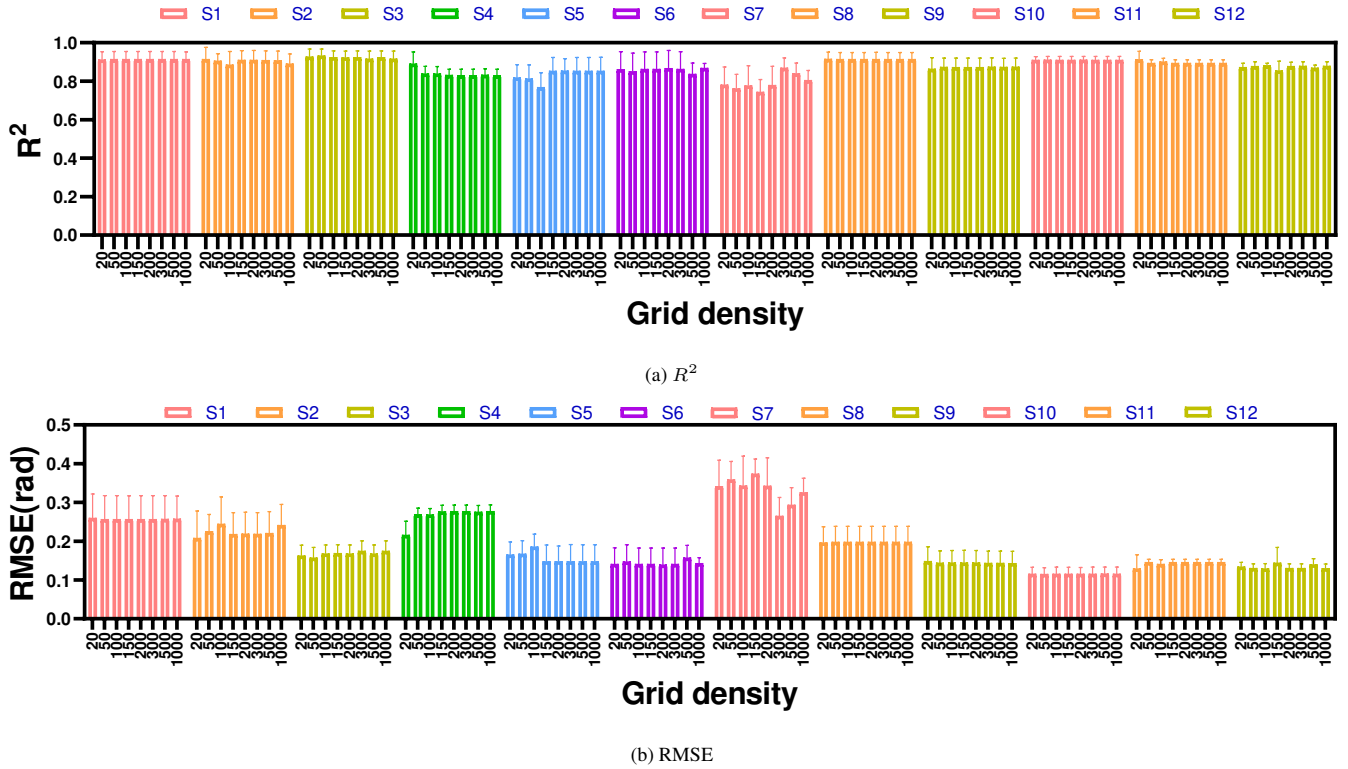


Fig. 6. The effects of number of grids on the estimation accuracy for each subject.

### B. Effects of Grid Density

To test the robustness of the proposed method against the grid densities, we evaluate the effects of the grid densities on the DC method. The grid densities result in the discretisation of the state and control variables in the solution processing. Different grid densities ( $Y = 20, 50, 100, 150, 200, 300, 500,$  and  $1000$ ) are evaluated. Fig.6 (a) and Fig. 6 (b) illustrate the  $R^2$  and RMSE for each subject at different grid densities. Different optimal solutions are found at different grid densities. For example, the estimation accuracy of S7 varies from 0.74 at grid 150 to 0.87 at grid 300 (also the optimisation duration for S7 is the longest in GA and DC). This is due to the influences of control variables in the proposed DC method, which contains the filtered EMG signals and MSK parameters. The filtered EMG signals interpret muscle recruitment information that may be contaminated by the noises, such as the electrode shift, crosstalk, and the impedance changes of electrode-skin interface [41]. Therefore, the DC method may converge to different optimal solutions. Nevertheless, the same estimation accuracy at different grid densities is found for most subjects, which indicates the proposed DC method is able to converge the same solution as the MSK parameters are time-independent.

Aside from the evaluation of the grid densities of the DC method, we further explore the impact of the sample frequencies on the baseline methods, according to [20], [42]. In this experiment, we estimate the optimised MSK parameters with the optimisation trial with 20 Hz, 50 Hz, 100 Hz, 200 Hz, 500 Hz, and 1000 Hz sample frequencies, via GA, SA, and PSO respectively. We further compare the results with the cor-

responding grid densities. Table III and Fig. 7 depict the mean  $R^2$  and RMSE across different sample frequencies. Results indicate that, at the higher sample frequencies (above 100 Hz), all four optimisation approaches are able to estimate the subject-specific parameters. In specific, PSO and DC show higher  $R^2$  than GA, followed by SA. Nevertheless, as shown in Fig. 7, at the low sample frequencies (20 Hz and 50 Hz respectively), baseline methods fail to identify the subject-specific parameters whereas the proposed DC method can find the optimal solution. The proposed approach maintains the same performance throughout different grid densities, which indicates its robustness. This is due to the fact that the proposed method employs system dynamics as constraints for parameter optimisation, i.e., activation dynamics, contraction dynamics, and the equation of motion. Fast optimisation is achieved by identifying the discretised parameters at all grid simultaneously.

In order to further investigate the effectiveness of the optimisation algorithms, the optimisation duration at the different grid densities or sample frequencies is measured. Fig. 8 depicts the linear regressions of the optimisation duration of four optimisation algorithms. The slopes are 0.636, 0.258, 0.426, and 0.263 for GA, SA, PSO, and DC respectively. Results reveal that GA has the largest computational cost to estimate the subject-specific parameters, followed by PSO. The computational costs of SA and DC are smaller than GA and PSO, and the computational cost of SA is close to the DC method. The proposed DC method, however, could estimate a better solution compared with SA, as elucidated in Table III. Moreover, the PSO shows a similar accuracy

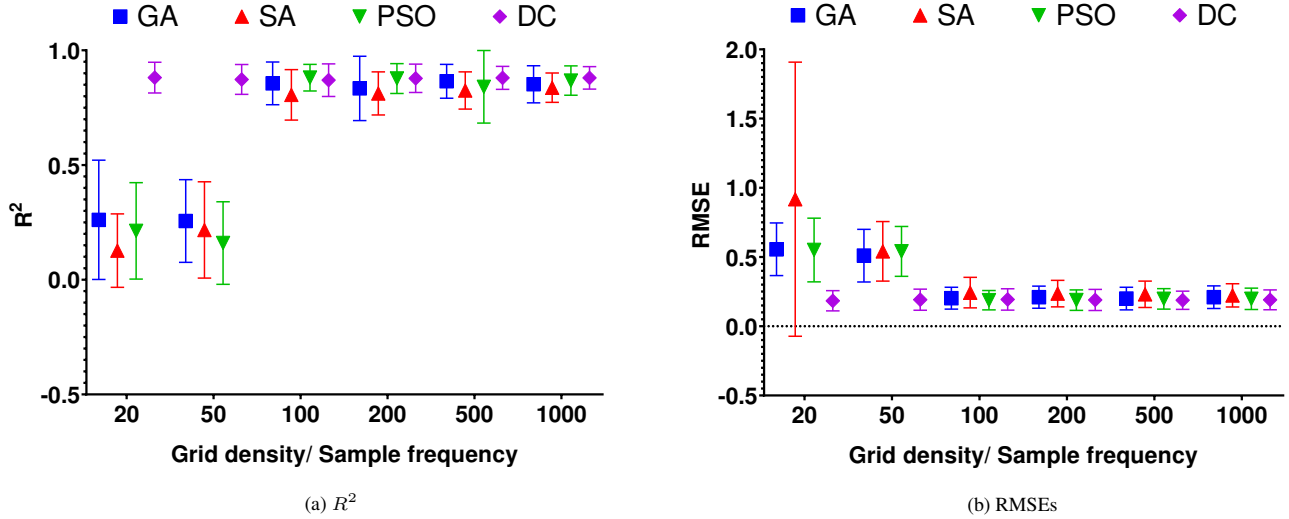


Fig. 7. The (a) mean  $R^2$  and (b) mean RMSE at different grid densities/sample frequencies. The proposed approach maintains the same estimation accuracy at lower grids whereas the baseline methods have the degraded estimation performance.

TABLE III  
MEAN ESTIMATION ACCURACY OF ALL OPTIMISATION ALGORITHMS OVER THE DIFFERENT GRID DENSITIES/SAMPLE FREQUENCIES

Genetic algorithm						
	20	50	100	200	500	1000
mean $R^2$	0.261( $\pm 0.26$ )	0.256( $\pm 0.18$ )	0.856( $\pm 0.093$ )	0.834( $\pm 0.14$ )	0.865( $\pm 0.074$ )	0.852( $\pm 0.081$ )
mean RMSE (rad)	0.556( $\pm 0.19$ )	0.510( $\pm 0.19$ )	0.203( $\pm 0.079$ )	0.210( $\pm 0.08$ )	0.200( $\pm 0.082$ )	0.210( $\pm 0.082$ )
Simulated Annealing						
	20	50	100	200	500	1000
mean $R^2$	0.127( $\pm 0.16$ )	0.217( $\pm 0.21$ )	0.806( $\pm 0.11$ )	0.812( $\pm 0.094$ )	0.825( $\pm 0.081$ )	0.837( $\pm 0.064$ )
mean RMSE (rad)	0.918( $\pm 0.99$ )	0.536( $\pm 0.215$ )	0.243( $\pm 0.11$ )	0.236( $\pm 0.096$ )	0.231( $\pm 0.095$ )	0.223( $\pm 0.084$ )
Particle Swarm Optimisation						
	20	50	100	200	500	1000
mean $R^2$	0.213( $\pm 0.21$ )	0.160( $\pm 0.18$ )	0.881( $\pm 0.058$ )	0.877( $\pm 0.065$ )	0.841( $\pm 0.158$ )	0.868( $\pm 0.064$ )
mean RMSE (rad)	0.551( $\pm 0.23$ )	0.541( $\pm 0.18$ )	0.188( $\pm 0.070$ )	0.189( $\pm 0.074$ )	0.198( $\pm 0.074$ )	0.198( $\pm 0.077$ )
Direct Collocation method						
	20	50	100	200	500	1000
mean $R^2$	0.881( $\pm 0.067$ )	0.873( $\pm 0.065$ )	0.870( $\pm 0.071$ )	0.878( $\pm 0.062$ )	0.880( $\pm 0.050$ )	0.880( $\pm 0.049$ )
mean RMSE (rad)	0.184( $\pm 0.073$ )	0.192( $\pm 0.076$ )	0.194( $\pm 0.077$ )	0.190( $\pm 0.076$ )	0.188( $\pm 0.066$ )	0.191( $\pm 0.072$ )

to DC but has a larger computational cost. Therefore, to a large extent, the DC method outperforms the state-of-the-art optimisation algorithms for the MSK model in terms of the estimation performance or computational effectiveness.

### C. Effects of different initial guesses

We further evaluate the effects of different initial guesses on the proposed DC method. The first initial guess is based on the nominal value, as shown in Table I. We choose the parameters optimised by the simulated annealing algorithm using 20 Hz as the second initial guess. Fig. 9 illustrates the estimation performance when two initial guesses are used. Results show that the proposed method is able to converge similar optimal solutions for most subjects. This indicates the robustness of the proposed method against the different initial guesses.

## IV. DISCUSSION

### A. Subject-specific Musculoskeletal Modelling

The MSK model is a powerful tool to understand the underlying neuromechanical processes and predict or simulate human motion with respect to the muscle activation. A generic MSK model, with the default or simply linear scaled physiological parameters, may be adequate to investigate the biomechanical questions that are not sensitive to the model personalisation [43]. For example, studying the muscle redundancy problem, investigating the biomechanical reactions to the physical interventions, or simulating the tendon transfer surgery could be achieved by a generic model appropriately. The subject-specific MSK model becomes necessary when it is coupled with the individual's neuromuscular quantities, such as a human-machine interface for assistive devices or the myoelectric control for prostheses. It is believed that the

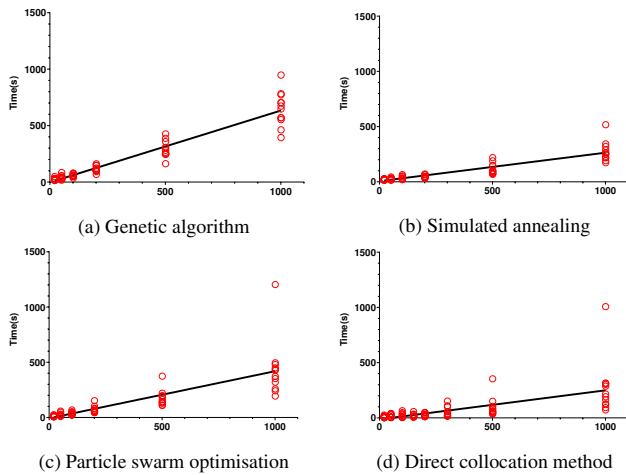


Fig. 8. Linear regressions of the optimisation duration at different grid densities/sample frequencies. The genetic algorithm shows the largest slope (0.636), followed by particle swarm optimisation (0.426). The simulated annealing algorithm has the similar slope with the direct collocation method (0.258 and 0.263 respectively), but results in poor solution among the optimisation algorithms.

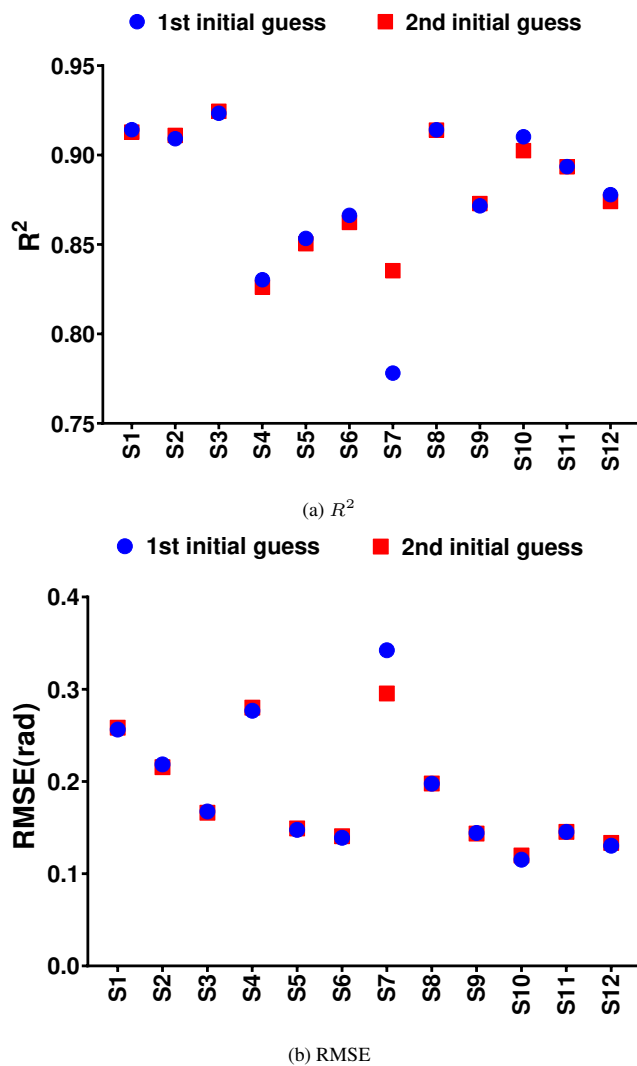


Fig. 9. Comparison of estimation accuracy when the different initial guesses are used.

subject-specificity enhances the physiological and physical plausibility so as to apply the MSK model to populations with muscular pathologies [44]. Furthermore, the subject-specific models can result in better motion estimation, as shown in Fig. 4.

The creation of subject-specific EMG-driven MSK models, however, requires the lengthy setup and time-consuming optimisation procedure, e.g., needs to multiple runs to select the most optimal solution. This is because the EMG-driven MSK models are mainly influenced by the EMG signals, the chosen optimisation algorithms, and the large number of physiological parameters [15]. In this study, we utilise the MATLAB optimisation toolbox to employ the evolutionary algorithms for parameter optimisation. The tolerance of all algorithms is set to  $1 \times 10^{-2}$ . Other optimisation criteria remain default. The experimental results show that all algorithms achieve the same level of estimation accuracy. The proposed DC method shows prominent performance given its ability to obtain the subject-specific parameter in an efficient manner. It is believed that the state-of-the-art optimisation algorithms are able to find the best solutions with different optimisation criteria and longer optimisation time, e.g., using the higher tolerance settings and different population size. However, the computational cost is increased accordingly. Recently, Kian *et al.* demonstrated that optimisation of the MSK models is task-dependent, which all experimental motion tasks may be considered as the optimisation trial to generate the subject-specific EMG-driven MSK model [45]. The augmented calibration sets substantially increase computational cost, leading to the use of MSK models in practical scenarios with the evolutionary algorithms being unrealistic. The proposed direct collocation method provides a computational-efficient solution to estimate the physiological parameters.

The highly personalised MSK model could be further achieved via magnetic resonance imaging (MRI), computed tomography (CT) scans, or the finite element model [46]–[50]. These approaches depend on the selection of anatomical landmarks from the MRI imaging technique and are independent of the dynamic movement trials of the participant. This encourages us to carry out future works that combine the imaging-based methods with the proposed DC method to generate more physiological-relevant MSK models.

### B. Direct Collocation method

The DC method for the MSK models has been widely explored recently, such as simulating the human pedalling [26], investigating the internal joint contact load during jumping [51], finding the optimal trajectories during the curved running [52], or identifying the stiffness for ankle-foot orthosis [53]. By transcribing the system dynamics into the large, sparse NLP problem and parametrising the control and states variables, the research questions can be solved efficiently due to the linear algebra operations [38]. Nevertheless, the direct collocation method requires the sparse constraints Jacobian matrix which is model-specific and task-dependent, leading to the generation of the Jacobian matrix being challenging and may be prone to errors. When studying a new research

question, a new Jacobian matrix is required. This issue can be addressed by the recently developed open source software, OpenSim Moco [54]. However, the models employed are mostly based on the linear scaled method, leading to estimation differences between the nature limb postures and model estimations [27]. To overcome this issue, we employ the direct collocation method to estimate the subject-specific parameters for the wrist MSK model by constraining the input control variables to the experimentally measured EMG signals and adding the physiological parameters to control variables. Fast optimisation is achieved by identifying the parameters at each grid simultaneously. The inclusion of parameters into control variables preserves the sparse pattern of the Jacobian matrix, as shown in Fig. 1. Although this study utilises the simplified version of the wrist MSK model, it shows the capabilities of providing the accurate wrist motion estimation, as demonstrated in Fig. 4 and Table II. Moreover, our goal is to enable the computational efficient optimisation to generate the personalised wrist MSK model, which is substantially demonstrated in this study.

### C. Limitations and Future work

There are several limitations to this study. Firstly, the proposed method is only validated on the wrist MSK model that involves one DoF. We solely utilise one motion task to optimise the wrist MSK model. Future work will be carried out employing the proposed method for the MSK model with increased complexities, i.e., more DoFs and motion tasks that span the upper limb. Secondly, the proposed method is demonstrated to estimate the subject-specific parameters for healthy subjects. Future work will evaluate the DC method for the MSK model with tendon compliance. Extending this study to patients with neurological disorders is also necessary to consider the abnormal muscle activation pattern and muscle weakness. Further studies will combine the proposed method with the MRI imaging technique to generate the wrist MSK model with higher personalisation.

## V. CONCLUSION

In this study, we proposed a computational efficient optimisation method to estimate subject-specific parameters of the wrist MSK model based on the direct collocation method. By adding the physiological parameters to control variables and inducing a specific constraint, we have demonstrated the feasibility of the proposed method to generate the personalised wrist MSK model with high estimation accuracy. Results show that the proposed DC method outperforms the state-of-the-art optimisation algorithms. We envision that the proposed method could alleviate the time-consuming optimisation procedure and facilitate the use of the MSK model in practical scenarios.

## REFERENCES

- [1] R.-E. Precup, T.-A. Teban, A. Albu, A.-B. Borlea, I. A. Zamfirache, and E. M. Petriu, "Evolving fuzzy models for prosthetic hand myoelectric-based control," *IEEE Trans. Instrum. Meas.*, vol. 69, no. 7, pp. 4625–4636, 2020.
- [2] C. G. McDonald, J. L. Sullivan, T. A. Dennis, and M. K. O'Malley, "A myoelectric control interface for upper-limb robotic rehabilitation following spinal cord injury," *IEEE Trans. Neural Syst. Rehabil. Eng.*, vol. 28, no. 4, pp. 978–987, 2020.
- [3] Q. Li, Z. Luo, and J. Zheng, "A new deep anomaly detection-based method for user authentication using multichannel surface EMG signals of hand gestures," *IEEE Trans. Instrum. Meas.*, vol. 71, pp. 1–11, 2022.
- [4] C. Shen, Z. Pei, W. Chen, J. Wang, J. Zhang, and Z. Chen, "Toward generalization of sEMG-based pattern recognition: a novel feature extraction for gesture recognition," *IEEE Trans. Instrum. Meas.*, vol. 71, pp. 1–12, 2022.
- [5] K. Gui, U.-X. Tan, H. Liu, and D. Zhang, "Electromyography-driven progressive assist-as-needed control for lower limb exoskeleton," *IEEE Trans. Med. Robot. Bionics.*, vol. 2, no. 1, pp. 50–58, 2020.
- [6] T. Bao, S. A. R. Zaidi, S. Xie, P. Yang, and Z.-Q. Zhang, "A CNN-LSTM hybrid model for wrist kinematics estimation using surface electromyography," *IEEE Trans. Instrum. Meas.*, vol. 70, pp. 1–9, 2020.
- [7] Y. Zhao, K. Qian, S. Bo, Z. Zhang, Z. Li, G.-Q. Li, A. A. Dehghani-Sanij, and S. Q. Xie, "Adaptive cooperative control strategy for a wrist exoskeleton using model-based joint impedance estimation," *IEEE/ASME Trans. Mechatronics*, pp. 1–10, 2022, doi:10.1109/TMECH.2022.3211671.
- [8] N. Lotti, M. Xiloyannis, F. Missiroli, C. Bokranz, D. Chiaradia, A. Frisoli, R. Riener, and L. Masia, "Myoelectric or Force control? a comparative study on a soft arm Exosuit," *IEEE Trans. Robot.*, vol. 38, no. 3, pp. 1363–1379, 2022.
- [9] A. Fleming, N. Stafford, S. Huang, X. Hu, D. P. Ferris, and H. H. Huang, "Myoelectric control of robotic lower limb prostheses: a review of electromyography interfaces, control paradigms, challenges and future directions," *J. Neural Eng.*, vol. 18, no. 4, p. 041004, 2021.
- [10] G. Hajian, E. Morin, and A. Etemad, "Multimodal estimation of endpoint force during quasi-dynamic and dynamic muscle contractions using deep learning," *IEEE Trans. Instrum. Meas.*, vol. 71, p. 2513111, 2022.
- [11] J. Berning, G. E. Francisco, S.-H. Chang, B. J. Fregly, and M. K. O'Malley, "Myoelectric control and neuromusculoskeletal modeling: Complementary technologies for rehabilitation robotics," *Curr. Opin. Biomed. Eng.*, vol. 19, p. 100313, 2021.
- [12] T. Bao, S. Q. Xie, P. Yang, P. Zhou, and Z. Zhang, "Towards robust, adaptive and reliable upper-limb motion estimation using machine learning and deep learning—a survey in myoelectric control," *IEEE J. Biomed. Health. Inform.*, vol. 26, no. 8, pp. 3822–3835, 2022.
- [13] M. K. Jung, S. Muceli, C. Rodrigues, A. Megía-García, A. Pascual-Valdunciel, A. J. Del-Ama, A. Gil-Agudo, J. C. Moreno, F. O. Barroso, J. L. Pons *et al.*, "Intramuscular EMG-driven musculoskeletal modelling: towards implanted muscle interfacing in spinal cord injury patients," *IEEE Trans. Biomed. Eng.*, vol. 69, no. 1, pp. 63–74, 2021.
- [14] K. J. Bennett, C. Pizzolato, S. Martelli, J. S. Bahl, A. Sivakumar, G. J. Atkins, L. B. Solomon, and D. Thewlis, "EMG-informed neuromusculoskeletal models accurately predict knee loading measured using instrumented implants," *IEEE Trans. Biomed. Eng.*, vol. 69, no. 7, pp. 2268–2275, 2022.
- [15] D. Soselia, R. Wang, E. M. Gutierrez-Farewik *et al.*, "Lower-limb joint torque prediction using LSTM neural networks and transfer learning," *IEEE Trans. Neural Syst. Rehabil. Eng.*, vol. 30, pp. 600–609, 2022.
- [16] W. Wang, W. Shi, Z.-G. Hou, B. Chen, X. Liang, S. Ren, J. Wang, and L. Peng, "Prediction of human voluntary torques based on collaborative neuromusculoskeletal modeling and adaptive learning," *IEEE Trans. Ind. Electron.*, vol. 68, no. 6, pp. 5217–5226, 2020.
- [17] C. Pozna, R.-E. Precup, E. Horvath, and E. M. Petriu, "Hybrid particle filter-particle swarm optimization algorithm and application to fuzzy controlled servo systems," *IEEE Trans. Fuzzy Syst.*, vol. 30, no. 10, pp. 4286–4297, 2022.
- [18] P. Silvestros, E. Preatoni, H. S. Gill, S. Gheduzzi, B. A. Hernandez, T. P. Holsgrove, and D. Cazzola, "Musculoskeletal modelling of the human cervical spine for the investigation of injury mechanisms during axial impacts," *PLoS one*, vol. 14, no. 5, p. e0216663, 2019.
- [19] Y. Zhao, Z. Zhang, Z. Li, Z. Yang, A. A. Dehghani-Sanij, and S. Xie, "An EMG-driven musculoskeletal model for estimating continuous wrist motion," *IEEE Trans. Neural Syst. Rehabil. Eng.*, vol. 28, no. 12, pp. 3113–3120, 2020.
- [20] R. M. Hinson, K. Saul, D. Kamper, and H. H. Huang, "Sensitivity analysis guided improvement of an electromyogram-driven lumped parameter musculoskeletal hand model," *J. Biomech.*, vol. 141, p. 111200, 2022.
- [21] I. A. Zamfirache, R.-E. Precup, R.-C. Roman, and E. M. Petriu, "Reinforcement learning-based control using Q-learning and gravitational search algorithm with experimental validation on a nonlinear servo system," *Inf. Sci.*, vol. 583, pp. 99–120, 2022.

- [22] M. Sartori, M. Reggiani, D. Farina, and D. G. Lloyd, "EMG-driven forward-dynamic estimation of muscle force and joint moment about multiple degrees of freedom in the human lower extremity," *PLoS one*, vol. 7, no. 12, p. e52618, 2012.
- [23] D. Simonetti, B. F. Koopman, and M. Sartori, "Clusterization of multi-channel electromyograms into muscle-specific activations to drive a subject-specific musculoskeletal model: towards fast and accurate clinical decision-making," in *2021 43rd Annual International Conference of the IEEE Engineering in Medicine & Biology Society (EMBC)*. IEEE, 2021, pp. 5979–5982.
- [24] D. Buongiorno, M. Barsotti, F. Barone, V. Bevilacqua, and A. Frisoli, "A linear approach to optimize an EMG-driven neuromusculoskeletal model for movement intention detection in myo-control: a case study on shoulder and elbow joints," *Front. Neurobot.*, vol. 12, p. 74, 2018.
- [25] T. Van Wouwe, L. H. Ting, and F. De Groot, "An approximate stochastic optimal control framework to simulate nonlinear neuromusculoskeletal models in the presence of noise," *PLoS Comput. Biol.*, vol. 18, no. 6, p. e1009338, 2022.
- [26] S. Park, G. E. Caldwell, and B. R. Umberger, "A direct collocation framework for optimal control simulation of pedaling using OpenSim," *Plos one*, vol. 17, no. 2, p. e0264346, 2022.
- [27] D. Blana, A. J. Van Den Bogert, W. M. Murray, A. Ganguly, A. Krasoulis, K. Nazarpour, and E. K. Chadwick, "Model-based control of individual finger movements for prosthetic hand function," *IEEE Trans. Neural Syst. Rehabil. Eng.*, vol. 28, no. 3, pp. 612–620, 2020.
- [28] A. Falisse, S. Van Rossum, I. Jonkers, and F. De Groot, "EMG-driven optimal estimation of subject-specific Hill model muscle–tendon parameters of the knee joint actuators," *IEEE Trans. Biomed. Eng.*, vol. 64, no. 9, pp. 2253–2262, 2016.
- [29] Y. Zhao, Z. Li, Z. Zhang, A. Asker, and S. Q. Xie, "A direct collocation method for optimization of EMG-driven wrist muscle musculoskeletal model," in *2021 IEEE International Conference on Robotics and Automation (ICRA)*. IEEE, 2021, pp. 1759–1765.
- [30] A. Wächter and L. T. Biegler, "On the implementation of an interior-point filter line-search algorithm for large-scale nonlinear programming," *Math. Program.*, vol. 106, no. 1, pp. 25–57, 2006.
- [31] D. Blana, E. K. Chadwick, A. J. van den Bogert, and W. M. Murray, "Real-time simulation of hand motion for prosthesis control," *Comput. Methods Biomech. Biomed. Engin.*, vol. 20, no. 5, pp. 540–549, 2017.
- [32] M. Millard, T. Uchida, A. Seth, and S. L. Delp, "Flexing computational muscle: modeling and simulation of musculotendon dynamics," *J. Biomech. Eng.*, vol. 135, no. 2, 2013.
- [33] T. S. Buchanan, D. G. Lloyd, K. Manal, and T. F. Besier, "Neuromusculoskeletal modeling: estimation of muscle forces and joint moments and movements from measurements of neural command," *J. Appl. Biomech.*, vol. 20, no. 4, p. 367, 2004.
- [34] Z. Li, Z. Huang, W. He, and C.-Y. Su, "Adaptive impedance control for an upper limb robotic exoskeleton using biological signals," *IEEE Trans. Ind. Electron.*, vol. 64, no. 2, pp. 1664–1674, 2016.
- [35] A. Seth, J. L. Hicks, T. K. Uchida, A. Habib, C. L. Dembia, J. J. Dunne, C. F. Ong, M. S. DeMers, A. Rajagopal, M. Millard *et al.*, "OpenSim: Simulating musculoskeletal dynamics and neuromuscular control to study human and animal movement," *PLoS Comput. Biol.*, vol. 14, no. 7, p. e1006223, 2018.
- [36] P. De Leva, "Adjustments to zatsiorsky-seluyanov's segment inertia parameters," *J. Biomech.*, vol. 29, no. 9, pp. 1223–1230, 1996.
- [37] D. L. Crouch and H. Huang, "Lumped-parameter electromyogram-driven musculoskeletal hand model: A potential platform for real-time prosthesis control," *J. Biomech.*, vol. 49, no. 16, pp. 3901–3907, 2016.
- [38] J. T. Betts, *Practical methods for optimal control and estimation using nonlinear programming*. SIAM, 2010.
- [39] K. R. Saul, X. Hu, C. M. Goehler, M. E. Vidt, M. Daly, A. Velisar, and W. M. Murray, "Benchmarking of dynamic simulation predictions in two software platforms using an upper limb musculoskeletal model," *Comput. Methods Biomech. Biomed. Engin.*, vol. 18, no. 13, pp. 1445–1458, 2015.
- [40] C. Y. Scovil and J. L. Ronsky, "Sensitivity of a hill-based muscle model to perturbations in model parameters," *J. Biomech.*, vol. 39, no. 11, pp. 2055–2063, 2006.
- [41] T. Bao, S. A. R. Zaidi, S. Xie, P. Yang, and Z.-Q. Zhang, "Inter-subject domain adaptation for CNN-based wrist kinematics estimation using semg," *IEEE Trans. Neural Syst. Rehabil. Eng.*, vol. 29, pp. 1068–1078, 2021.
- [42] L. Pan, D. L. Crouch, and H. Huang, "Comparing emg-based human-machine interfaces for estimating continuous, coordinated movements," *IEEE Trans. Neural Syst. Rehabil. Eng.*, vol. 27, no. 10, pp. 2145–2154, 2019.
- [43] D. J. Saxby, B. A. Killen, C. Pizzolato, C. Carty, L. Diamond, L. Modenese, J. Fernandez, G. Davico, M. Barzan, G. Lenton *et al.*, "Machine learning methods to support personalized neuromusculoskeletal modelling," *Biomech. Model. Mechanobiol.*, vol. 19, no. 4, pp. 1169–1185, 2020.
- [44] R. Akhundov, D. J. Saxby, L. E. Diamond, S. Edwards, P. Clausen, K. Dooley, S. Blyton, and S. J. Snodgrass, "Is subject-specific musculoskeletal modelling worth the extra effort or is generic modelling worth the shortcut?" *PLoS one*, vol. 17, no. 1, p. e0262936, 2022.
- [45] A. Kian, C. Pizzolato, M. Halaki, K. Ginn, D. Lloyd, D. Reed, and D. Ackland, "The effectiveness of EMG-driven neuromusculoskeletal model calibration is task dependent," *J. Biomech.*, vol. 129, p. 110698, 2021.
- [46] C. Ye, Y. Wang, and Y. Tao, "High-density large-scale TMR sensor array for magnetic field imaging," *IEEE Trans. Instrum. Meas.*, vol. 68, no. 7, pp. 2594–2601, 2018.
- [47] W. Kong, Q. Miao, and Y. Lei, "Multimodal sensor medical image fusion based on local difference in non-subsampled domain," *IEEE Trans. Instrum. Meas.*, vol. 68, no. 4, pp. 938–951, 2018.
- [48] C. Klemt, D. Nolte, Z. Ding, L. Rane, R. A. Quest, M. E. Finnegan, M. Walker, P. Reilly, and A. M. Bull, "Anthropometric scaling of anatomical datasets for subject-specific musculoskeletal modelling of the shoulder," *Ann. Biomed. Eng.*, vol. 47, no. 4, pp. 924–936, 2019.
- [49] C. Pizzolato, V. B. Shim, D. G. Lloyd, D. Devaprakash, S. J. Obst, R. Newsham-West, D. F. Graham, T. F. Besier, M. H. Zheng, and R. S. Barrett, "Targeted achilles tendon training and rehabilitation using personalized and real-time multiscale models of the neuromusculoskeletal system," *Front. Bioeng. Biotechnol.*, vol. 8, p. 878, 2020.
- [50] H. Kainz, M. Wesseling, and I. Jonkers, "Generic scaled versus subject-specific models for the calculation of musculoskeletal loading in cerebral palsy gait: Effect of personalized musculoskeletal geometry outweighs the effect of personalized neural control," *Clin. Biomech.*, vol. 87, p. 105402, 2021.
- [51] S. Porsa, Y.-C. Lin, and M. G. Pandy, "Direct methods for predicting movement biomechanics based upon optimal control theory with implementation in OpenSim," *Ann. Biomed. Eng.*, vol. 44, no. 8, pp. 2542–2557, 2016.
- [52] M. Nitschke, E. Dorschky, D. Heinrich, H. Schlarb, B. M. Eskofier, A. D. Koelewijn, and A. J. van den Bogert, "Efficient trajectory optimization for curved running using a 3D musculoskeletal model with implicit dynamics," *Sci. Rep.*, vol. 10, no. 1, pp. 1–12, 2020.
- [53] M. Sreenivasa, M. Millard, M. Felis, K. Mombaur, and S. I. Wolf, "Optimal control based stiffness identification of an ankle-foot orthosis using a predictive walking model," *Front. Hum. Neurosci.*, vol. 11, p. 23, 2017.
- [54] C. L. Dembia, N. A. Bianco, A. Falisse, J. L. Hicks, and S. L. Delp, "Opensim moco: Musculoskeletal optimal control," *PLoS Comput. Biol.*, vol. 16, no. 12, p. e1008493, 2020.